

Sympathetic cooling of $\text{NH}(X^3\Sigma^-)$ molecules by Rb and Cs atoms at ultralow energies

Mario Tacconi, Enrico Bodo, and Franco A. Gianturco*

Department of Chemistry, University of Rome La Sapienza, Piazzale A. Moro 5, 00185 Rome, Italy

(Received 18 July 2006; revised manuscript received 28 September 2006; published 10 January 2007)

The relative size of the elastic cross sections between NH molecules colliding with Cs and Rb atoms on the lowest potential energy surfaces of spin-stretched quartet symmetry are computed using the full quantum treatment and taking the target molecule to be in its ground rotational state. Results are compared between the two systems under similar dynamics and the Rb atom is found to yield larger cross sections at ultralow energies. The process is seen to be dominated by dispersion interaction and an analysis of the effects on the cross sections induced by changes on the C_6 coefficients is carried out in detail for both systems.

DOI: [10.1103/PhysRevA.75.012708](https://doi.org/10.1103/PhysRevA.75.012708)

PACS number(s): 34.50.-s, 34.50.Bw

I. INTRODUCTION

Recent experimental advances in cooling and trapping of cold atoms have stimulated research for the creation of cold molecules [1,2]. The availability of cold and ultracold molecules may open up many new applications such as condensation of complex molecular systems, coherent control of molecular collisions in ultracold chemistry, and precision measurements of molecular interactions. In the past decade, several methods have been developed to cool and trap molecules at cold and ultracold temperatures. The helium buffer gas-cooling technique [3] has proven to be effective in loading molecules into a magnetic trap [4] and it has been shown to be a method that may be used to create cold molecular beams [5]. Such a molecular beam, in conjunction with an atomic condensate, could be used to investigate atom-molecule collisions at cold and ultracold temperatures. Another approach for the production of ultracold molecules involves photoassociation of laser-cooled atoms [6–9], which generally yields molecules with translational temperatures in the μK regime. However, molecules created by this technique are in highly excited vibrational levels and collisional quenching of these molecules limits their lifetimes. A similar approach using a magnetic field (magnetoassociation) has been successful in creating molecular Bose-Einstein condensates (BECs) of fermionic atoms using the Feshbach resonance technique [10–13]. The resulting molecules are also highly vibrationally excited as in the photoassociation technique but they are more stable against collisional decay due to the Pauli blocking. For polar molecules, the Stark decelerator method [14–16] has proven to be very useful. It uses a time-varying electric field to slow molecules and it is applicable to a broad range of molecular systems with permanent dipole moments. Applications of this technique to cool and trap metastable CO [14], deuterated ammonia [17], as well as the OH radical [18] have been demonstrated. The possibility to cool and trap molecules provides an unique opportunity to study collisions between atoms and molecules at very low translational energies. Schemes to produce diatomic molecules in highly excited rotational states have also been pro-

posed [19,20] and recently realized [21]. Theory has suggested that the collisional dynamics of such internally hot molecules would be particularly interesting at low temperatures where quantum-mechanical effects play a dominant role and the collision dynamics is very sensitive to the intermolecular interaction potential and the relative separation of the initial and final internal energy levels of the scattering partners [22–26].

Since translational temperatures typically reach the mK or μK regimes or lower, the internal energy may be orders of magnitude larger by comparison and therefore, the exchange of internal energy during a collision is an important issue in cold and ultracold physics: the inelastic cross sections were shown to follow an inverse velocity dependence at very low initial kinetic energies of the incident atom in accordance with the Wigner threshold law [27]. Since cold and ultracold collisions are very sensitive to intermolecular interaction, accurate potential surfaces for the scattering complexes are very important for reliable theoretical simulations of energy transfer. This is therefore one of the reasons why, in the present examples, we intend to focus on the collisional cooling of an open-shell target such as $\text{NH}(X^3\Sigma^-)$ interacting with Rb or Cs atoms at ultralow energies: the scope the work is thus directly linked with the detailed knowledge which we need to acquire on the relevant molecular interactions forces. In particular, the open-shell nature of the systems involved requires the inclusion of a fairly accurate representation of static and dynamical correlation effects, together with the description of several potential energy surfaces (PESs) associated with various spin multiplicities of the overall system. This means that the quantum dynamics associated with the collisional energy transfer between cold atomic beams of Cs and Rb with NH molecular targets must necessarily rely on an accurate representation of such interaction and must further analyze the effects of changes in the potential onto the scattering attributes: both aspects of the problem will be dealt with by the present work. The following section will briefly describe our interaction potentials, since they have already been given in greater detail in a recent publication [28], and indicate our choice in the dynamical analysis, while Sec. IV will report the quantum dynamics and the sensitivity of it from changes in the long-range forces. Our present conclusions will be given in Sec. V.

*Corresponding author. FAX: +39-06-49913305; Electronic address: fa.gianturco@caspur.it

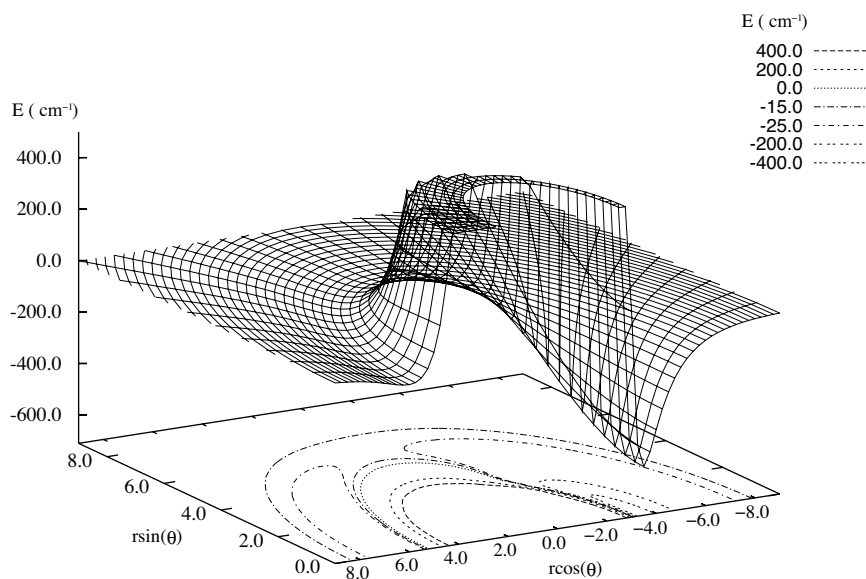


FIG. 1. Computed quartet symmetry potential-energy surface for the $\text{NH}(X^3\Sigma^-)\text{-Rb}(^2S_{5s})$ system. The deep well associated with the N side is shown on the right side of the figure.

II. INTERACTION POTENTIAL

We are initially considering the $\text{NH}(X^3\Sigma^-)$ target molecule to be a rigid rotor and therefore the resulting PESs are two-dimensional objects given as a function of orientation θ and center-of-mass distance R : the $\theta=0^\circ$ orientation corresponds to the atomic approach on the H side of the molecule. We defined an evenly spaced grid in θ with $\Delta\theta=10^\circ$ while the discrete 80 points representation of the R coordinate was obtained using a variable step size ΔR . Therefore 1520 points of the PESs have been computed using the complete active space self-consistent field (CASSCF) approach [29] and the internally contracted multireference configuration interaction (MRCI) wave function [30]. Furthermore, in order to reduce the computational effort and to model the relativistic effects of the core electrons, the heavy alkali-metal atoms have been described via an effective core potential (ECP), while the Gaussian basis set for the NH molecule was taken to be the cc-aug-vTZ in its uncontracted form [31]. The chosen ECP was the scalar relativistic small core ECPxMWB implemented by the Stuttgart group [32]: the details of the methodology of our calculations have been already given in Ref. [28]. The semiquantitative analysis of the various possible asymptotic states carried out there showed that the electronic states of the alkali-NH complexes, which arise from the ionic dissociation limit, strongly characterize the electronic structure of these systems and therefore it is natural to treat as relevant in our study both such ionic states and the neutral ones, which lie below the ionic dissociation limit. In the selection of the active orbitals space we therefore made the choices discussed already in Ref. [28]. We further discovered that the situation of the quartet electronic states is much simpler because no diabatic crossings (or conical intersections) between the doublet (ionic) electronic states and the quartet (neutral) electronic states occur and that this feature allowed for a reduction of the active orbitals space by eliminating the higher-energy $(n-1)d$ orbitals of the alkali-atom and the π^* orbitals of the NH [28]. The full quartet interactions could therefore be accurately

described and their analytic representations obtained by using the two-center expansion already discussed earlier by us [33]; we further generated all the bound states supported by both systems for the $J=0$ total angular momentum [28]. Because the quartet states of both systems are energetically away from the more complicated crossings that occur for the doublet states of the complexes, one can safely assume that the very-low energy dynamics that we are interested in could be handled rather realistically by using the latter PESs independently from the others. Furthermore, in order to represent the all-important dispersion interaction in each complex, we generated in our fitting procedure a long-range part, which simply reads as $-C_6/R^6$, with the coefficients determined from the actual numerical behavior of each PES for each atomic partner. A pictorial view of the surfaces is given by Figs. 1 and 2, for the Rb and the Cs atomic partner, respectively. Both surfaces are available on request from the authors. Both computed PESs reveal a very strong orientational anisotropy in the sense that their lowest attractive wells are both located at the nitrogen side of the target molecule, with only a weak dispersion-driven well on the H side of the latter. The strength of the interactions is also fairly similar in both systems, although the Rb partner shows the deeper minimum at around 570 cm^{-1} , to be compared with the value for Cs at around 480 cm^{-1} .

III. COMPUTATIONAL APPROACH

Coupled differential or integrodifferential equations arise naturally in the quantum mechanical formulation of the inelastic and reactive scattering processes whenever one looks for the time-independent scattering eigenstates of a system, here denoted as $\Psi^{i,+}$. For weakly interacting species this state is usually expanded in terms of diabatic target eigenstates

$$\Psi^{i,+}(\mathbf{R}, \mathbf{x}) = \sum_f F_{i \rightarrow f}(\mathbf{R}) X_f(\mathbf{x}), \quad (1)$$

where i labels collectively the initial state of the colliding partners and the X_f are the eigenstates of the isolated mol-

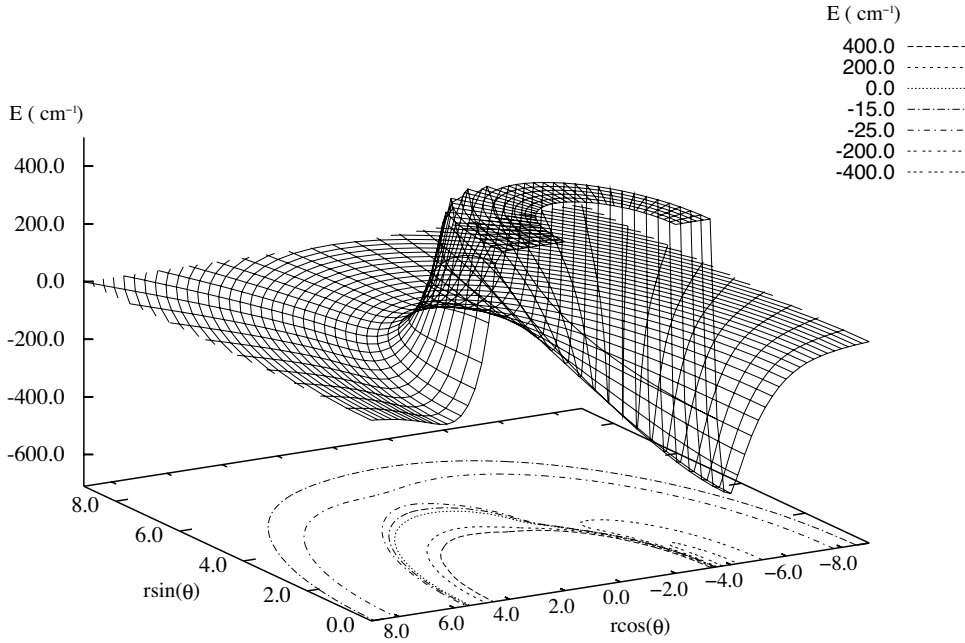


FIG. 2. Same calculations as those of Fig. 1 but here referring to the NH($X^3\Sigma^-$)-Cs($^2S_{6s}$) complex.

ecules (channel eigenstates) with internal coordinates denoted by \mathbf{x} . The $F_{i \rightarrow f}$ are the channel components of the scattering wave function that depend on the interparticle distance \mathbf{R} and which have to be determined by solving the usual radial Schrödinger equation

$$\left\{ \frac{d^2}{dR^2} + \mathbf{k}^2 - \mathbf{V}(R) - \frac{\mathbf{I}^2}{R^2} \right\} \mathbf{F}(R) = 0, \quad (2)$$

where $[\mathbf{k}^2]_{ij} = \delta_{ij} 2\mu(E - \epsilon_i)$ is the diagonal matrix of the asymptotic (squared) wave vectors and $[\mathbf{I}^2]_{ij} = \delta_{ij} l_i(l_i + 1)$ is the matrix representation of the square of the orbital angular momentum operator. Finally, $\mathbf{V}(R) = 2\mu\mathbf{U}(R)$ is the potential coupling matrix, which depends on the angular momenta involved. To efficiently solve Eq. (2) we have implemented over the year a new algorithm based on the multichannel variable phase equation [34], which is particularly useful in the presence of long-range potentials [35]. One therefore performs separate calculations for each J value so that, given a certain initial molecular total angular momentum N , the s -wave calculation with $l=0$ is given for total angular momentum value $J=N$. The numerical implementation of the close-coupling scheme obviously depends on the specific values of the spin and other angular momenta involved in the collision processes. The total quenching cross section for a molecule, which initially is in the N rovibrational state, is obtained as a sum over the various total angular momenta of the relevant T matrix elements

$$\sigma(N \rightarrow N', E_i) = \frac{\pi}{(2N+1)k_N^2} \sum_J (2J+1) \times \sum_{l=|J-N|}^{J+N} \sum_{l'=|J-N'|}^{J+N'} |T_{Nl \rightarrow N'l'}^J|^2, \quad (3)$$

with all indices being the same in the case of elastic processes.

IV. RESULT AND DISCUSSION

A. Elastic cross sections

As mentioned at the beginning, one of the aims of the present work is to establish the comparable capabilities of Rb and Cs atoms in providing collisional cooling of NH molecular partners at ultralow scattering energies. To this end, we have carried out calculations which, at least initially, treat the NH molecule coupled to the incoming atoms without taking into account the additional effects of the spin rotation and the weak spin-spin terms in the Hamiltonian. While we expect that such a simplification should not substantially affect the elastic cross sections, we intend to implement the correct coupling Hamiltonian in a later study of rotationally inelastic collisions for the present systems [36]. The present calculations therefore describe the NH target as a $^1\Sigma$ rigid rotor in its $j=0$ level. We coupled several rotational channels up to $j_{max}=25$ and carried out the outer integration up to $R_{max}=300 \text{ \AA}$. The calculation was done for the case $J=0$ and $l=0$ in the low-energy regime. All the convergence parameters were finally varied until cross-section values remained within a confidence threshold of about 1%. The elastic cross sections, as a function of collision energies in the ultracold regime, are reported by Fig. 3 for both complexes. The following considerations could be readily made:

(1) The systems are clearly reaching the Wigner regime of the dynamics below about 10^{-3} cm^{-1} since at those energies both elastic cross sections tend to a constant;

(2) The Rb atoms show an elastic cross section, which is about five times larger than that for the Cs atom: the two interaction potentials have also been shown to follow the same trend in the sense that Cs-NH was seen before as a weaker interaction with respect to the Rb-NH potential-energy surface;

(3) Both elastic cross sections become very large in value as soon as the linear regime is attained in the ultralow energy calculations. Hence, we could say that both systems are ex-

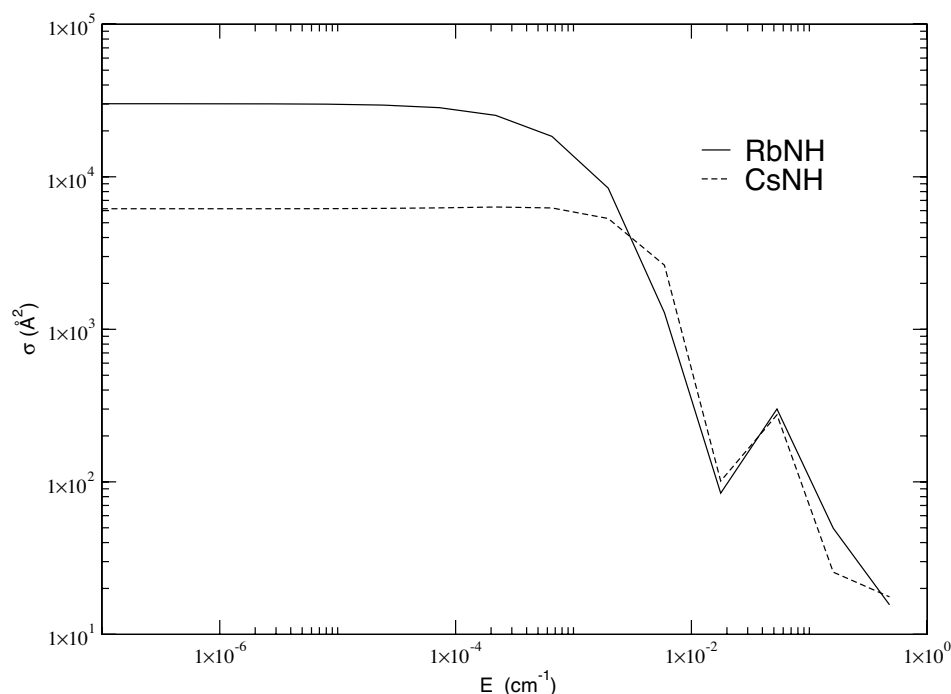


FIG. 3. Computed elastic s -wave cross sections at ultralow energies for Rb (solid line) and Cs (dashed) interacting with NH through the spin-stretched quartet states.

pected to act as good *coolant* for molecular NH in contact with cold Rb and Cs atoms.

B. Effect of the dispersion terms

To further explore the reliability of the previous results in the sense of testing their sensitivity with respect to potential changes, we start from the well-known fact that the dispersion interactions are crucial components of the full PES when one needs to evaluate low and ultralow-energy collisional attributes [37]. On the other hand, reliable values of C_6 and C_8 coefficients for molecular systems are very few and far apart, and additionally with very little information on their angular dependence or general anisotropy [38]. In the present study we have obtained our C_6 coefficients from numerical extrapolation of our *ab initio* values and therefore we decided to check what effects on the final cross sections would be caused by changing the dominant C_6 coefficient within a realistic range of its values. The panels of Fig. 4 indicate, for each system, how the long-range tails are modified by varying C_6 within a range of one order of magnitude around the initial estimates from the potential fit of the present study. One sees there that such changes only affect the long-range tails of our interactions since the well regions and the repulsive ones, also shown in the panels of Fig. 4, are essentially unchanged.

Additional information at vanishing collision energies can be obtained by examining the behavior of the real part of the scattering length [22–25] via the corresponding expansion of the elastic matrix elements in powers of k ,

$$S_{jj'} = 1 + 2i\delta_j(k) = 1 - 2ik(\alpha_j - i\beta_j) = 1 - 2ika_j. \quad (4)$$

It allows us to obtain the real (α_j) and imaginary (β_j) parts of the scattering length a_j , which is in turn related, in the same limit of vanishing k , to the elastic cross section

$$\sigma_j^{el} = 4\pi|a_j|^2. \quad (5)$$

By analyzing the behavior of a_j we can therefore see how its value and sign relate to the features of the scattering potential. In the present dynamics, therefore, adjustments of the overall interaction correspond to changes of the long-range part of the potential, i.e., to variations of the dominant C_6 coefficients for both the present systems. The calculations reported by Fig. 5 examine, for the case of the RbNH complex, the behavior of three different scattering attributes related to such changes. The latter corresponds to both weaker potentials (smaller C_6 values) and stronger interactions (larger C_6 values) with respect to the best fit, marked by circles and arrows in each of the panels. One interesting result is provided by the behavior of the scattering length reported by the central panel. One sees there that such a quantity is slightly positive and small for the initial potential and corresponds to a complex (M -NH) very weakly bound (see the bottom panel in the same figure). When one now reduces the potential strength going to smaller C_6 values, one sees that the scattering length increases and then diverges when forming zero-energy resonances of the samples. These resonances further convert into virtual states as the scattering length becomes negative. By the same token, when the potential strength is increased, the stronger interaction binds the complex even further and brings down from the continuum a second zero-energy resonance (second divergence in the middle panel), which then evolves into another bound state supported by the yet stronger PES as C_6 increases. The effect on the computed cross sections, reported in the top panel of Fig. 5, is also rather striking and follows the *tuning* of the potential strength attained by changes of the dispersion coefficients. Thus, we see that the elastic cross sections reach larger values at the formation of a zero-energy resonant state (for a diverging scattering length) and further decrease to

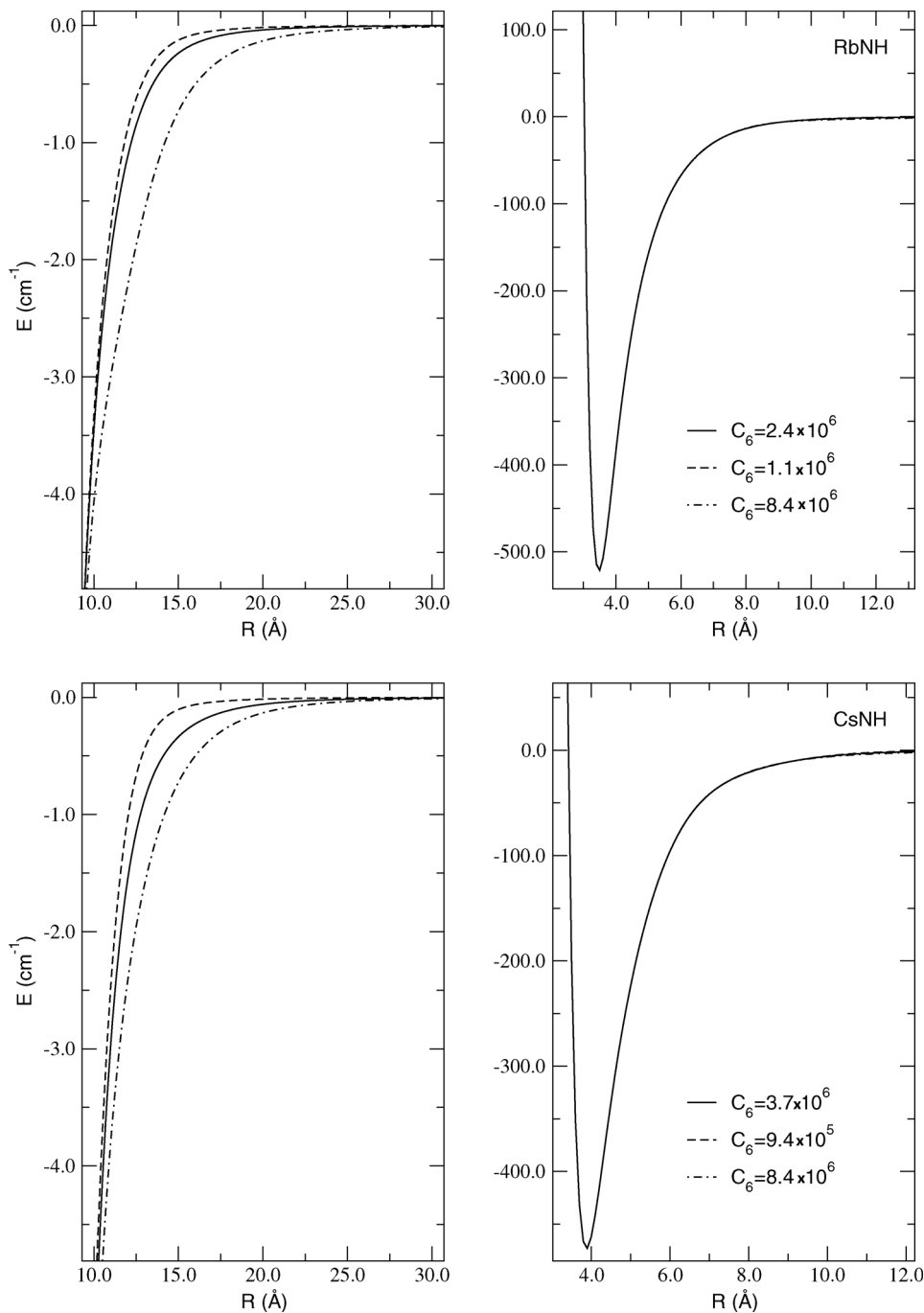


FIG. 4. Computed interactions along the $\theta=180^\circ$ direction and with varying values of the dispersion coefficients C_6 , included in the long-range parts. Upper panels: results for the RbNH system; lower panels: same as for the CsNH system; the spin-stretched quartet states.

minimum values when the scattering length changes sign and then goes through zero: a situation that corresponds to the appearance of the Ramsauer-Townsend (RT) minimum in the elastic cross section since the corresponding s -wave phase shift goes through π [39]. Since we do not really have an external way of evaluating the quality of the initial dispersion terms in the interaction, we see that to treat them as *tuning knobs* for controlling the strength of the collisional coupling allows us to induce remarkable changes in the behavior of the corresponding scattering observables. Thus, a range of changes for C_6 of less than one order of magnitude causes the system to undergo the formation of either additional virtual states or new threshold resonances, which strongly modify the size and behavior of the elastic colli-

sions. The results, which we report by Fig. 6 for the CsNH complex, follow a very similar behavior and confirm the appearance of both marked maxima or RT minima in the relevant elastic cross sections at vanishing collision energies.

V. PRESENT CONCLUSION

The work described has dealt with the evaluation of the elastic cross section at ultralow energies for collision of Rb and Cs atoms with $\text{NH}(X^3\Sigma^-)$ molecules at ultralow collision energies. The systems were considered to interact via their lowest potential energy surfaces, which are associated with the spin-stretched arrangements of the quartet states in both systems. In such arrangements, in fact, no conical intersec-

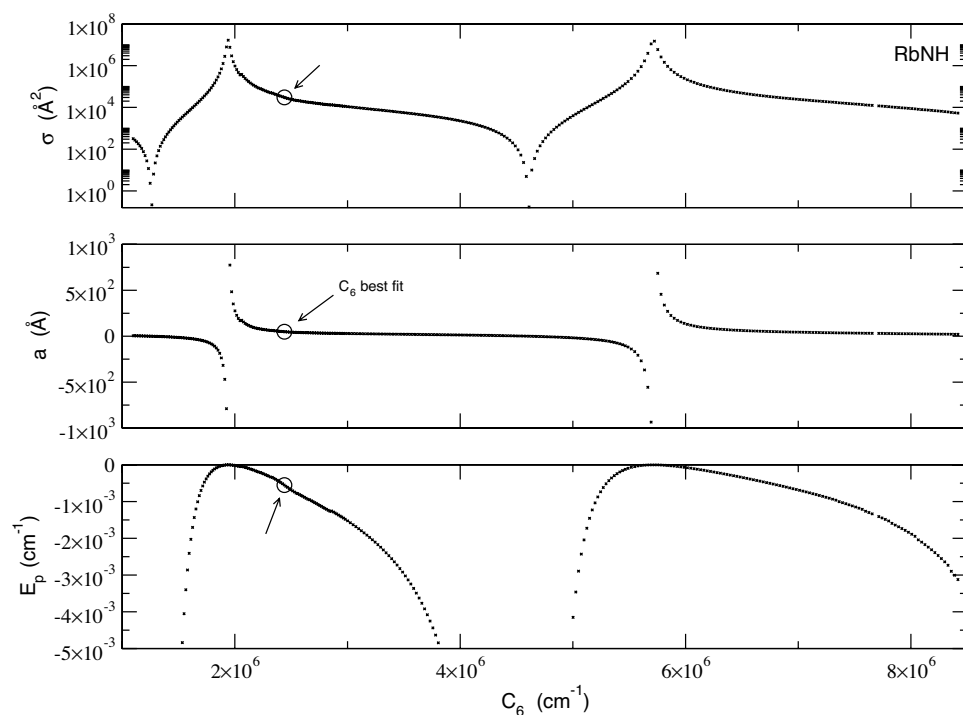


FIG. 5. RbNH system: computed elastic cross sections (top panel), real part of the scattering length (middle panel), and energies of the virtual or bound states as a function of the strength of the dispersion interaction.

tions are present with higher states and therefore the ultracold dynamics can be realistically treated as occurring along simpler PESs. The latter were calculated from highly correlated wave functions and have been discussed in some detail in Sec. II of the present manuscript. The scattering calculations were carried out using the spaced-fixed, coupled-channel approach involving the target rotational states and disregarding for the time being both vibrational effects and spin-rotation coupling contributions. The results indicate that the elastic cross sections are fairly large at the nanokelvin

regimes and therefore suggest, provided one can trust the computed potentials, efficient sympathetic cooling on the part of both cold atoms when interacting with the NH molecule. They also indicate that Rb atoms have elastic cross sections, which are about five times larger than the case of the Cs partner. We have also carried out a numerical sensitivity study based on the analysis of changes in the leading dispersion coefficient C_6 , which causes corresponding changes of scattering attributes at ultralow energies. In particular, we have analyzed the size modifications in the elastic

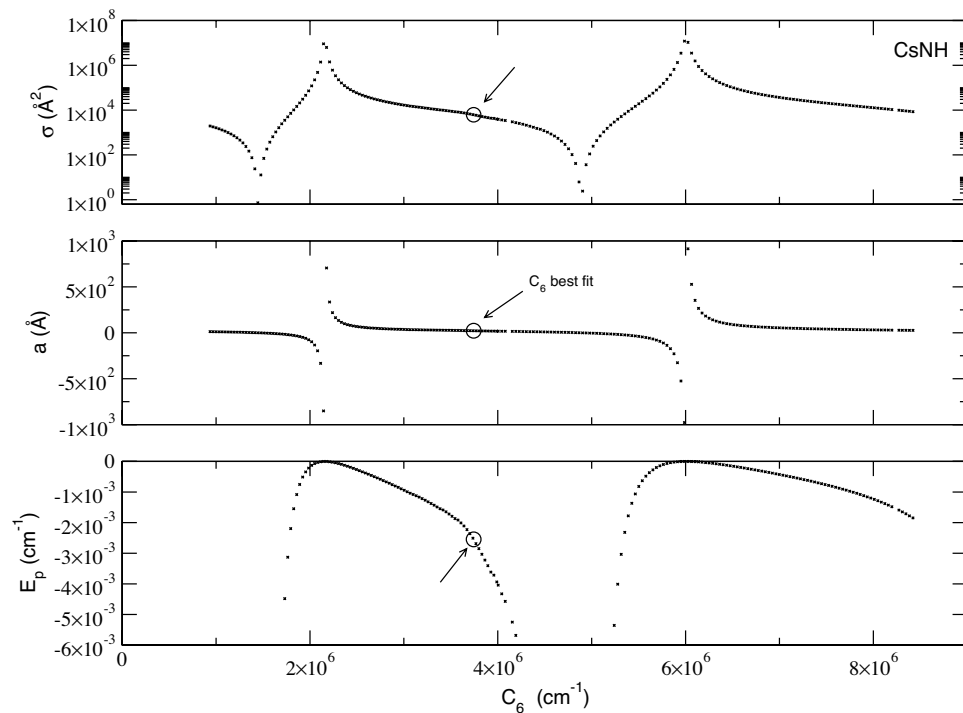


FIG. 6. Same calculations as those reported by Fig. 5 but this time for the CsNH system.

cross sections over a range of realistic variations of the dispersion interactions in both systems. The calculations led to the following results:

(1) At ultralow collision energies all scattering attributes are very sensitive functions of the long-range forces and markedly depend on their values. This is one of the consequences of the quantum suppression features at ultralow energies.

(2) In both systems small changes of the C_6 coefficients cause the scattering length to go through a divergence and therefore generate the appearance of zero-energy resonances where the cross sections increase in size by orders of magnitude.

(3) The strengthening of the interaction potential causes additional long-range weakly bound states and also shows the presence of Ramsauer-Townsend minima in the cross sections, where the s -wave phase shift goes through zero (or

π) and the associated scattering length changes from positive to negative, producing on its evolution a divergent behavior with a virtual state (zero-energy resonance) formation.

In other words, the calculations suggest that the true molecular potentials located somewhere along the choices we made for the dispersion coefficients should be capable of causing very dramatic effects from scattering experiments at ultralow energies and that such effects may be large enough to be amenable to experimental detection.

ACKNOWLEDGMENTS

The financial support of The University Research Committee at *La Sapienza* in Rome and of the European Network *Comol* (Grant No. HPRN-CT-2002-00290) are gratefully acknowledged. We also thank Dr. L. Sanchez-Gonzales for useful discussion on the scattering coding.

-
- [1] J. Doyle, R. Krems, and F. Masnou-Seeuws, *Eur. Phys. J. D* **31**, 149 (2004).
- [2] R. Krems, *Int. Rev. Phys. Chem.* **24**, 99 (2005).
- [3] J. Doyle, R. Krems, J. Kim, and D. Patterson, *Phys. Rev. A* **52**, R2515 (1995).
- [4] J. Weinstein, R. deCarvalho, T. Guillet, B. Friedrich, and J. Doyle, *Nature (London)* **395**, 148 (2002).
- [5] D. Egorov, T. Lahaye, W. Schollkopf, B. Friedrich, and J. Doyle, *Phys. Rev. A* **66**, 043401 (2002).
- [6] A. Fioretti, D. Comparat, A. Crubellier, O. Dulieu, F. Masnou-Seeuws, and P. Pillet, *Phys. Rev. Lett.* **80**, 4402 (1998).
- [7] A. Nikolov, E. Eyler, X. Wang, H. Wang, J. Li, W. Stwalley, and P. Goulp, *Phys. Rev. Lett.* **82**, 703 (1999).
- [8] R. Wynar, R. Freeland, D. Han, C. Ryu, and D. Heinzen, *Science* **287**, 1016 (2000).
- [9] W. C. Stwalley and Y. H. Uang, *J. Mol. Spectrosc.* **195**, 194 (1999).
- [10] M. Greiner, C. A. Regal, and D. S. Jin, *Nature (London)* **426**, 537 (2003).
- [11] M. W. Zwierlein, C. A. Stan, C. H. Schunck, S. M. Raupach, S. Gupta, Z. Hadzibabic, and W. Ketterle, *Phys. Rev. Lett.* **91**, 250401 (2003).
- [12] C. A. Regal, M. Greiner, and D. S. Jin, *Phys. Rev. Lett.* **92**, 040403 (2004).
- [13] M. Bartenstein, A. Altmeyer, S. Riedl, S. Jochin, C. Chin, J. H. Denschlag, and R. Grimm, *Phys. Rev. Lett.* **92**, 120401 (2004).
- [14] H. L. Bethlem, G. Berden, and G. Meijer, *Phys. Rev. Lett.* **83**, 1558 (1999).
- [15] H. L. Bethlem, G. Berden, F. M. H. Crompvoets, R. T. Jongma, A. J. A. Roji, and G. Meijer, *Nature (London)* **406**, 491 (2000).
- [16] H. L. Bethlem and G. Meijer, *Int. Rev. Phys. Chem.* **22**, 73 (2003).
- [17] F. M. H. Crompvoets, H. L. Bethlem, J. Kupper, A. J. A. van Roij, and G. Meijer, *Phys. Rev. A* **69**, 063406 (2004).
- [18] S. Y. T. van de Meerakker, P. H. M. Smeets, N. Vanhaecke, R. T. Jongma, and G. Meijer, *Phys. Rev. Lett.* **94**, 023004 (2005).
- [19] J. Karczmarek, J. Wright, P. Corkum, and M. Ivanov, *Phys. Rev. Lett.* **82**, 3420 (1999).
- [20] J. Li, J. T. Bahns, and W. C. Stwalley, *J. Chem. Phys.* **112**, 6255 (2000).
- [21] D. M. Villeneuve, S. A. Aseyev, P. Dietrich, M. Spanner, M. Y. Ivanov, and P. B. Corkum, *Phys. Rev. Lett.* **85**, 542 (2000).
- [22] N. Balakrishnan, R. C. Forrey, and A. Dalgarno, *Chem. Phys. Lett.* **280**, 1 (1997).
- [23] N. Balakrishnan, R. C. Forrey, and A. Dalgarno, *Phys. Rev. Lett.* **80**, 3224 (1998).
- [24] E. Bodo, F. A. Gianturco, and A. Dalgarno, *J. Phys. B* **35**, 4075 (2002).
- [25] E. Bodo, F. Sebastianelli, E. Scifoni, F. A. Gianturco, and A. Dalgarno, *Phys. Rev. Lett.* **89**, 283201 (2002).
- [26] E. Bodo, F. A. Gianturco, and A. Dalgarno, *Chem. Phys. Lett.* **353**, 127 (2002).
- [27] E. P. Wigner, *Phys. Rev.* **73**, 1002 (1948).
- [28] M. Tacconi, E. Bodo, and F. A. Gianturco, *Theor. Chem. Acc.* (to be published).
- [29] H.-J. Werner and P. J. Knowles, *J. Chem. Phys.* **82**, 5053 (1985).
- [30] P. J. Knowles and H.-J. Werner, *Chem. Phys. Lett.* **145**, 514 (1988).
- [31] P. Soldan and J. Hutson, *Phys. Rev. Lett.* **92**, 163202 (2004).
- [32] T. Leininger, *Chem. Phys. Lett.* **255**, 274 (1996).
- [33] E. Bodo, F. A. Gianturco, and E. Yurtsever, *J. Low Temp. Phys.* **138**, 259 (2005).
- [34] A. Degasperis, *Nuovo Cimento* **34**, 1667 (1964).
- [35] R. Martinazzo, E. Bodo, and F. A. Gianturco, *Comput. Phys. Commun.* **151**, 187 (2003).
- [36] M. Tacconi, E. Bodo, and F. A. Gianturco (unpublished).
- [37] M. Marinescu, H. R. Sadeghpour, and A. Dalgarno, *Phys. Rev. A* **49**, 982 (1994).
- [38] A. Derevianko, W. R. Johnson, M. S. Safranov, and J. F. Babb, *Phys. Rev. Lett.* **82**, 3589 (1999).
- [39] Roger G. Newton, *Scattering Theory of Waves and Particles*, 2nd ed. (Springer-Verlag, New York, 1982).